Supramolecular Chemistry

Aromatic Foldamer Helices as α-Helix Extended Surface Mimetics

Márton Zwillinger,[a, b] Post Sai Reddy,[c, d] Barbara Wicher,[e] Pradeep K. Mandal,[d] Márton Csékei,[a] Lucile Fischer,[c] András Kotschy,*[a] and Ivan Huc*[d]

Abstract: Helically folded aromatic oligoamide foldamers have a size and geometrical parameters very distinct from those of α-helices and are not obvious candidates for α-helix mimicry. Nevertheless, they offer multiple sites for attaching side chains. It was found that some arrays of side chains at the surface of an aromatic helix make it possible to mimic extended α-helical surfaces. Synthetic methods were developed to produce quinoline monomers suitably functionalized for solid phase synthesis. A dodecamer was prepared. Its crystal structure validated the initial design and showed helix bundling involving the α-helix-like interface. These results open up new uses of aromatic helices to recognize protein surfaces and to program helix bundling in water.

Protein–protein interactions (PPIs) often involve α-helices as key, if not the only, components of the binding interface.[1] Great effort has thus been devoted to develop α-helix mimetics as PPI competitive inhibitors[2] all the way to the clinic.[3] This includes methods to enhance α-helix conformational stability through macrocycles involving main chain or side chain functionalities;[3,4] the use of conformational templates and helix stabilizing monomers;[5] or the design of peptidic analogues or homologues that adopt helical conformations more stable than α-helices of similar length.[6] In those cases, side chains may be displayed on all faces of the helix. In contrast, other α-helix mimetics consist of more or less rigid linear scaffolds, for example, terphenyl,[7] aromatic amides,[8] oxopiperazines,[9] pyrrolinone-pyrrolidine,[10] carrying proteinogenic side chains at distance intervals similar to those of an α-helix, typically following the *i*, *i*+4, *i*+7 arrangement. The functionalization of these scaffolds on opposite edges to include other side chain positions has also been proposed.[11] All these mimics have distinct degrees of freedom and may not perfectly reproduce a desired side chain arrangement, yet they represent good starting points for rational design. Here, we introduce the concept that helical aromatic foldamers may provide original solutions to α-helix mimicry, even in the case of long helices.

Foldamers with aryl rings in their main chain may adopt stable helical conformations in solution.[12] These helices feature a pitch of 3.5 Å and a diameter of at least 1.3 nm that do not relate to those of an α-helix. They can be decorated with proteinogenic side chains and may interact with protein surfaces[13] but, at first sight, they appear to be unsuitable for α-helix mimicry (see Figure 1 in ref. [14]). Instead, some have been used as duplex B-DNA charge surface mimetics.[15] Nevertheless, aromatic foldamers possess many sites for functionalization and thus for creating diverse side chain patterns.

Oligoamides of δ-peptidic 8-amino-2-quinolinecarboxylic acid Q adopt helical conformations with 2.5 units per turn (Figure 1a,b).[16] Q_n helices have until now been built with low side chain density, mainly in position 4,[13,14,16] occasionally in position 5,[15,17] and not in position 6. Upon careful examination of the Q_n helix (Figure S1), we realized that a simple side chain arrangement involving 4- and 6-functionalized quinoline rings potentially matches with that of the face of an α-helix. The actual curvature of α-helices may vary between the ideal 3.6_{13} α-helix, with 3 turns for 11 residues (Figure 1d), and the more classical 3.6_{13} α-helix with 5 turns for 18 units (Figure 1e, Figure S2).[18] We found that one can match four side chains (*i*, *i*+3, *i*+4, *i*+7) of a 3.6_{13} α-helix and four residues on a *P*-helical aromatic backbone with an RMSD of 0.70–0.95 Å (Figure 1e), which fares well compared to reported values.[8e] The match can be extended to eight side chains (the above plus *i*+11, *i*+14, *i*+15, *i*+18)—an entire face—of an octadecapeptide (Fig-

[a] M. Zwillinger, Dr. M. Csékei, Dr. A. Kotschy
Servier Research Institute of Medicinal Chemistry
Záhony utca 7. Budapest, 1031 (Hungary)
E-mail: andras.kotschy@servier.com

[b] M. Zwillinger
Hevesy György PhD School of Chemistry
Eötvös Loránd University
Budapest (Hungary)

[c] Dr. P. S. Reddy, Dr. L. Fischer
CNRS, Bordeaux Institut National Polytechnique
CBMN (UMR 5248), IECB
Université de Bordeaux
2 rue Robert Escarpit, 33600 Pessac (France)

[d] Dr. P. S. Reddy, Dr. P. K. Mandal, Prof. Dr. I. Huc
Department of Pharmacy and Center for Integrated Protein Science
Ludwig-Maximilians-Universität
Butenandtstr. 5–13, 81377 München (Germany)
E-mail: ivan.huc@cup.lmu.de
Homepage: https://huc.cup.uni-muenchen.de/

[e] Dr. B. Wicher
Department of Chemical Technology of Drugs
Poznan University of Medical Sciences
Grunwaldzka 6, 60780 Poznan (Poland)

Supporting information and the ORCID identification numbers for the authors of this article can be found under: https://doi.org/10.1002/chem.202004064.

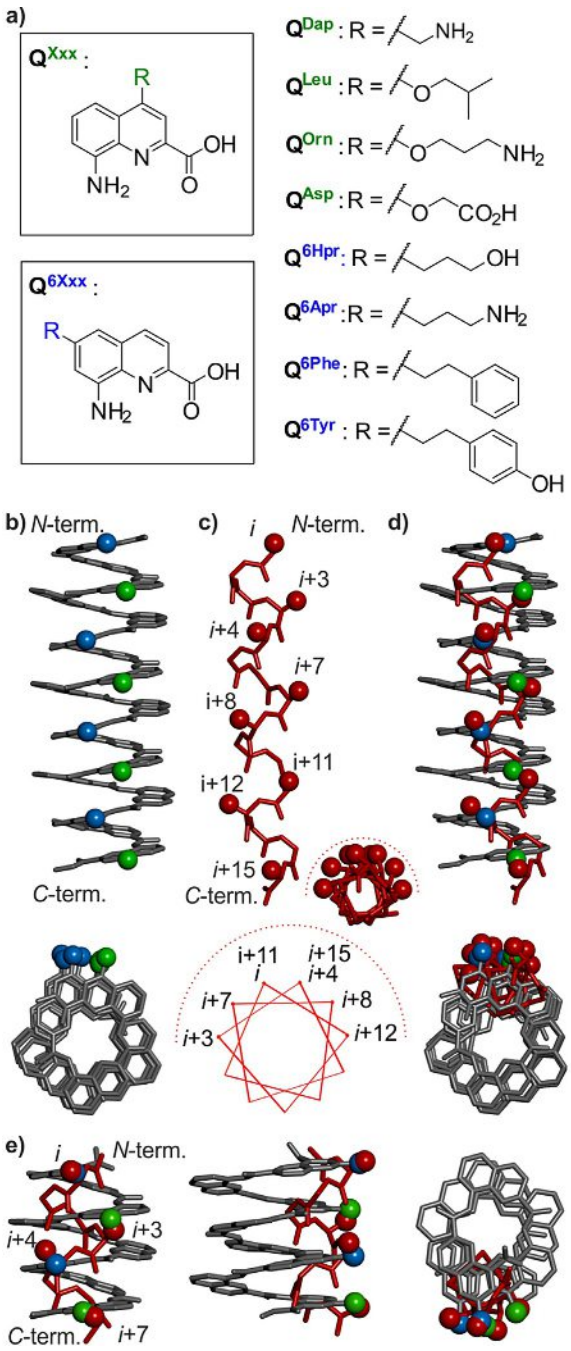

Figure 1. a) Some previously described 4-substituted Q^{Xxx} monomers and some of the new 6-substituted Q^{6Xxx} monomers reported in this study. b) Molecular model and helical wheel of a $(Q^{6Xxx}QQ^{Xxx}Q_2)_3Q^{6Xxx}QQ^{Xxx}$ octadeca-arylamide helix showing substituents in position 6 and 4 as blue and green balls, respectively. c) Structure of an ideal (computed) 3.66_{13} α-helical hexadecapeptide with β-carbons shown as red spheres. d) Overlay of the side chains in b) and c) with an RMSD of 1.50 Å (see Figure S2). e) Overlay of four side chains of $Q^{6Xxx}QQ^{Xxx}Q_2Q^{6Xxx}QQ^{Xxx}$ (same color code as b) with four side chains of a short 3.6 α-helix (red spheres). Note the position of the side chains in the 3.6 helix slightly differ from those of the 3.66 helix above. An RMSD of 0.92 Å is calculated if the overlay concerns the peptide β-carbon and a quinoline exocyclic carbon in position 4 or 6 (shown). An RMSD of 0.79 Å is calculated if the overlay concerns the peptide α-carbon and the quinoline endocyclic carbon in position 4 or 6 (not shown).

ure S2). Of note, side chains on the α-helix face that are consecutive in the peptide sequence are matched by residues separated by two units in the quinoline helix. For a 3.66_{13} α-helix, eight side chains may be matched as well (Figure 1 b–d) but, due to the difference in curvature, the peptide side chains involved are not all the same (for the last four: $i+8$, $i+11$, $i+12$, $i+15$). In the case of eight side chains, the match shows imperfections (RMSD of 1.5 Å) but these may be acceptable in so far that not all side chains may be required, and also that structural parameters may vary in both quinoline helices and α-helices through induced fit. Additionally, reverting helix N- to C-polarity, inverting handedness, or both, offer slight variations of side chain positions (e.g. swap 4- and 6-substituents) and enhance the possibility to find a suitable match (Figure S3). For example, slightly decreasing helix curvature may reduce or increase the distance between side chains within the array depending on the side chains concerned, but this effect is reversed when inverting helix handedness (note that the handedness of long aromatic helices in water is kinetically inert). Furthermore, side chain match may be improved by shifting some of them to position 5 of the quinoline ring (Figure S4). Of course, aromatic helices remain much larger than an α-helix and may not fit in a narrow protein groove. But PPIs mediated by a single α-helix face represent the most frequent scenario,[1] and an aromatic helix would fit in such cases. In addition, aromatic helices possess other useful features such as resistance to proteolytic degradation and cell penetration capabilities.[14,19]

To exploit the new design, we first needed a robust synthetic route to 6-functionalized monomers suitably protected for solid phase synthesis. The eight monomers **1a**–**h** shown in Scheme 1 were targeted, which bear protected hydrophobic, polar neutral and cationic side chains. The synthetic route relies on key intermediates **2** and **3**, which were obtained on a multigram scale. Compound **2** was prepared in three steps from commercially available 4-bromo-2-nitroaniline (see Supporting information) and **3** in two steps from **2**. These initial steps were all chromatography-free and scalable. Both **2** and **3** bear different halogen atoms at C-4 and C-6. Selective functionalization at C-6 was achieved, but this route also makes it possible to further functionalize position 4 if additional side chains are required, that is, in both positions 4 and 6 of the same quinoline ring. Depending on the nature of the side chain and availability of the corresponding synthons, regioselective reactions at C-6 involved sp^2–sp^2 (Suzuki), sp^2–sp^3 (Suzuki) or sp^2–sp (Sonogashira) cross-couplings. Side chains could thus be introduced having a C–C triple, C–C double or C–C single bond. We therefore had the choice of a wide range of potential coupling conditions. The loop through trifluoroacetamido intermediate **3** was required because the nitro function was found to be incompatible with certain sp^2–sp^3 Suzuki couplings. For that, the nitro group was carefully reduced over Raney-Ni without dehalogenation prior to trifluoroacetylation.

With commercial or easily available alkyne precursors, Sonogashira couplings were first attempted. Conditions, particularly the temperature, were optimized for each coupling to enhance regioselectivity. While **4a**–**d** were obtained in satisfactory yields, it was not the case with benzylacetylene. Instead, the phenylpropenyl side chain of **4e** was introduced in fair yield

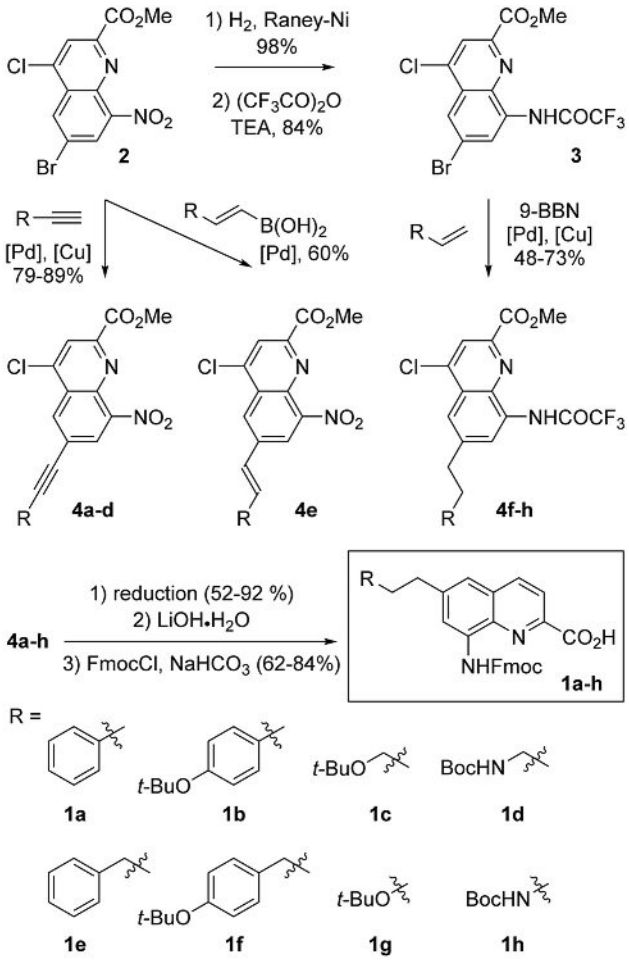

Scheme 1. General synthetic strategy of 6-substituted quinoline amino acid building blocks **1a–h** with protected proteinogenic side chains suitable for solid phase foldamer synthesis (SPFS). 9-BBN: 9-borabicyclo[3.3.1]nonane.

through an sp^2-sp^2 Suzuki coupling using the commercially available boronic acid. Another approach was developed where acetylene or vinyl boronate precursors would have been difficult to obtain. The corresponding alkenes were hydroborated to yield alkylboranes quantitatively, which were directly utilized in a one-pot, sp^2–sp^3 Suzuki coupling with **3** to obtain **4f–h**. In the case of **4f** the alkene precursor was synthesized in one step (see supporting information). Conditions were optimized in each case to obtain good selectivity and suppress dehalogenation.

Following side chain installation, the double (or triple) bond was saturated, the nitro group was reduced, and the aryl-Cl bond was hydrogenolized in the same hydrogenation step. Optimization and screening were required to find ideal conditions. Eventually, $HCOONH_4$ proved to be an excellent transfer hydrogenation agent and, in most cases, side reactions were suppressed. Finally, methyl ester and trifluoroacetamide hydrolysis followed by Fmoc installation afforded **1a–h** on a 0.57–1.30 g scale. The final products were purified by normal phase flash chromatography and preparative RP-HPLC to reach the desired purity (>99%) for solid phase foldamer synthesis.

Sequence **5** (Figure 2a) was designed to validate side chain positions using the new Q^{6Xxx} monomers and to possess some side chain diversity (eight different aromatic monomers). Manual solid phase synthesis[20] provided outstanding crude purity (Figure 2b). The spreading of ^1H NMR signals of aromatic amide protons in $[D_6]$DMSO (Figure 2c) is characteristic of helix folding. Derivative **6** was prepared to have a slightly better water solubility and was set to crystallize from water/acetoni-

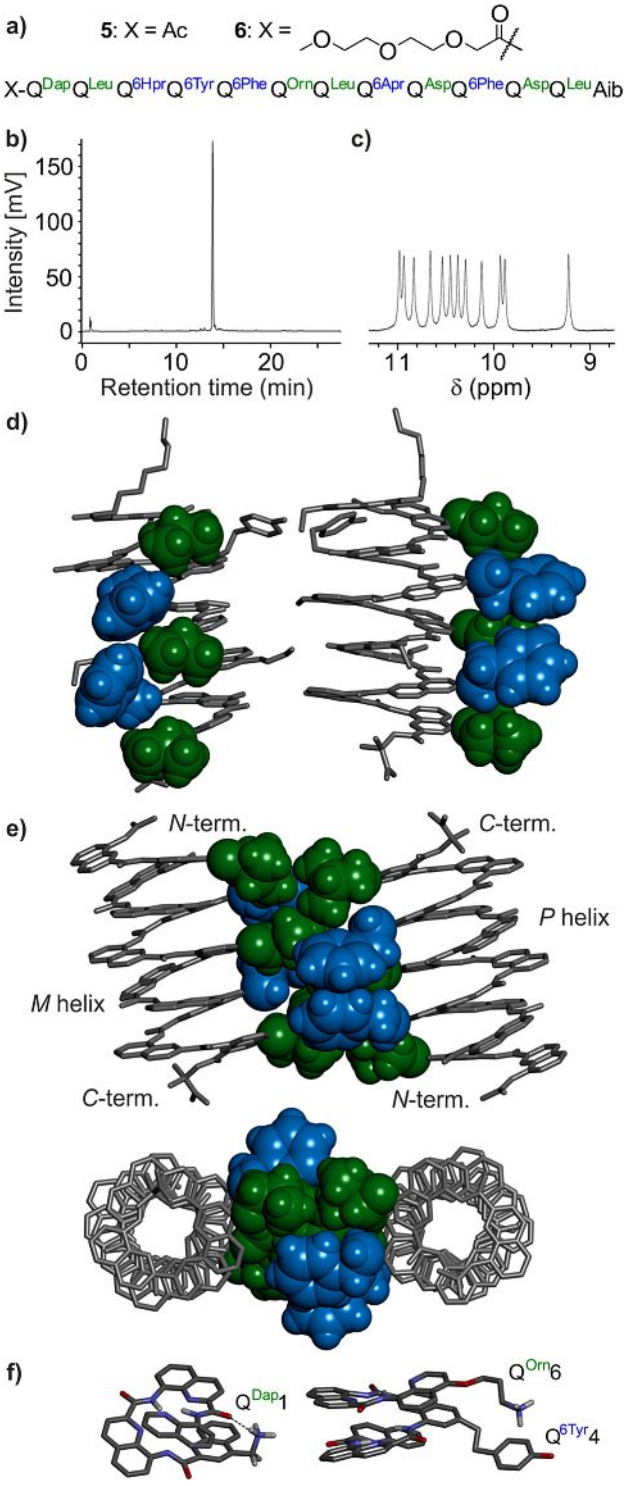

Figure 2. a) Sequences **5** and **6**. b) Crude C18 RP-HPLC profile of **5**. c) Part of the ^{1}H NMR spectrum of crude **5** in [D_6]DMSO showing the expected twelve aromatic amide resonances. Data for purified samples are shown in the Supporting Information. d)–f) Crystal structure of **6**. Deposition number 2014258 contains the supplementary crystallographic data for this paper. These data are provided free of charge by the joint Cambridge Crystallographic Data Centre and Fachinformationszentrum Karlsruhe Access Structures service. d) Views showing the side chains of $Q^{Leu}2$, $Q^{6Phe}5$, $Q^{Leu}7$, $Q^{6Phe}10$ and $Q^{Leu}12$ in CPK view with the same color code as in Figure 1 b. The rest of the structure is shown in grey tubes. e) Views of a discrete dimer with interdigitated hydrophobic side chains (same residues as in d). f) Side chain-main chain hydrogen bonding involving the ammonium of $Q^{Dap}1$ and an amide carbonyl oxygen atom ($d_{N\text{-}O}$ = 2.83 Å), and side chain-side chain proximity between $Q^{Orn}6$ and $Q^{Tyr}4$. Note the ammonium group of $Q^{Orn}6$ was placed at a hypothetical position as, unlike the three carbons of the side chain, it cannot be located in the electron density map. Some hydrogen atoms are shown at calculated positions but were not included during refinement. Solvent molecules have been removed for clarity.

trile using the hanging drop method. Crystals that diffracted up to a resolution of 1.2 Å were obtained and the structure was solved in the *P*-1 space group with two independent molecules in the asymmetric unit (Figure 2 d-2f). Figure 2 d shows an array of hydrophobic Q^{Xxx} and 6-substituted Q^{6Xxx} monomer side chains arranged as predicted in Figure 1 b. An overlay with the predicted model demonstrates an RMSD of 0.4 Å of the first atom of each side chain, establishing the good prediction of side chain positions by a simple molecular modelling tool, and the weak deviation of the structure of **6** from an ideal calculated helix (Figure S5). Furthermore, pairs of parallel helices are observed in which two arrays of hydrophobic groups cluster and interdigitate (Figure 2 e), as in α-helix peptide bundles.[21] The two helices nevertheless have opposite handedness and opposite N→C polarity, an assembly mode that has already been observed in helix bundles.[22] In solution, water rich samples only show broad ^{1}H NMR lines (Figure S5), suggesting that no well-defined aggregate prevails. Nevertheless, the structure of **6** clearly hints at the possibility to design knob-into-hole complementary hydrophobic interfaces similar to those of α-helices. Notwithstanding a certain disorder of the side chains resulting in partial occupancy factors, additional remarkable features of this structure include likely side chain-main chain hydrogen bonding (Figure 2 f left) and also some proximity between Orn and 6Tyr side chains hinting at possible intramolecular cation-π interactions (Figure 2 f right). Side chain-side chain interactions are indeed well-known to influence α-helix stability.[23] Q_n helices are intrinsically very stable and need no further stabilization. Nevertheless, such interactions would help to fine-tune the stability of related sequences having stronger dynamics.[24]

Altogether, these results establish the suitability of substituted Q_n oligomers as scaffolds to mimic some extended arrays of side chains at the surface of long α-helices. Interestingly, sequences that combine Q monomers and α-amino acids do not provide such a good match.[25] Prospective applications of these mimics include the recognition of protein surfaces and the construction of peptide bundles. Progress in these directions is being made in our laboratories and will be reported in due course.

Acknowledgements

Part of this research has been implemented in the frame of the project FIEK_16-1-2016-0005 "Development of molecular biomarker research and service center", with the support provided from the National Research, Development and Innovation Fund of Hungary, financed under the FIEK_16 funding Scheme. This work was also supported by the European Union (H2020-MSCA-IF-2016-751019-PROFOLIG, postdoctoral fellowship to P.S.R.). It benefited from the facilities and expertise of the Biophysical and Structural Chemistry platform at IECB, CNRS UMS3033, INSERM US001, Université de Bordeaux. We thank Marine Stupfel for preliminary contributions and Daniel Bindl for assistance with NMR measurements. Synchrotron data were collected at beamline P13 operated by EMBL Hamburg at the PETRA III storage ring (DESY, Hamburg, Germany). We thank Saravanan Panneerselvam for assistance in using the beamline. Open access funding enabled and organized by Projekt DEAL.

Conflict of interest

The authors declare no conflict of interest.

Keywords: aromatic foldamers · peptidomimetics · structure based design · structure elucidation · α-helix

[1] a) B. N. Bullock, A. L. Jochim, P. S. Arora, *J. Am. Chem. Soc.* **2011**, *133*, 14220–14223; b) A. L. Jochim, P. S. Arora, *ACS Chem. Biol.* **2010**, *5*, 919–923.

[2] a) V. Azzarito, K. Long, N. S. Murphy, A. J. Wilson, *Nat. Chem.* **2013**, *5*, 161–173; b) A. J. Wilson, *Chem. Soc. Rev.* **2009**, *38*, 3289; c) J. M. Davis, L. K. Tsou, A. D. Hamilton, *Chem. Soc. Rev.* **2007**, *36*, 326–334; d) M. Pelay-Gimeno, A. Glas, O. Koch, T. N. Grossmann, *Angew. Chem. Int. Ed.* **2015**, *54*, 8896–8927; *Angew. Chem.* **2015**, *127*, 9022–9054; e) L.-G. Milroy, T. N. Grossmann, S. Hennig, L. Brunsveld, C. Ottmann, *Chem. Rev.* **2014**, *114*, 4695–4748.

[3] V. Guerlavais, C. Elkin, H. M. Nash, T. K. Sawyer, B. J. Graves, E. Feyfant, WO/2013/123266, **2013**.

[4] a) G. L. Verdine, G. J. Hilinski, *Methods Enzymol.* **2012**, *503*, 3–33; b) T. A. Hill, N. E. Shepherd, F. Diness, D. P. Fairlie, *Angew. Chem. Int. Ed.* **2014**, *53*, 13020–13041; *Angew. Chem.* **2014**, *126*, 13234–13257; c) L. D. Walensky, *Science* **2004**, *305*, 1466–1470; d) A. Jamieson, N. Robertson, *Rep. Org. Chem.* **2015**, 65.

[5] a) Y. Demizu, M. Doi, M. Kurihara, H. Okuda, M. Nagano, H. Suemune, M. Tanaka, *Org. Biomol. Chem.* **2011**, *9*, 3303; b) C. Toniolo, G. M. Bonora, A. Bavoso, E. Benedetti, B. di Blasio, V. Pavone, C. Pedone, *Biopolymers* **1983**, *22*, 205–215; c) G. R. Marshall, E. E. Hodgkin, D. A. Langs, G. D. Smith, J. Zabrocki, M. T. Leplawy, *Proc. Natl. Acad. Sci. USA* **1990**, *87*, 487–491; d) J. P. Schneider, J. W. Kelly, *Chem. Rev.* **1995**, *95*, 2169–2187; e) J. Fremaux, L. Mauran, K. Pulka-Ziach, B. Kauffmann, B. Odaert, G. Guichard, *Angew. Chem. Int. Ed.* **2015**, *54*, 9816–9820; *Angew. Chem.* **2015**, *127*, 9954–9958; f) L. Mauran, B. Kauffmann, B. Odaert, G. Guichard, *Compt. Rendus Chim.* **2016**, *19*, 123–131; g) J. Maury, B. A. F. Le Bailly, J. Raftery, J. Clayden, *Chem. Commun.* **2015**, *51*, 11802–11805; h) D. S. Kemp, T. P. Curran, J. G. Boyd, T. J. Allen, *J. Org. Chem.* **1991**, *56*, 6683–6697; i) D. S. Kemp, T. P. Curran, W. M. Davis, J. G. Boyd, C. Muendel, *J. Org. Chem.* **1991**, *56*, 6672–6682.

[6] a) M. Werder, H. Hauser, S. Abele, D. Seebach, *Helv. Chim. Acta* **1999**, *82*, 1774–1783; b) T. Sawada, S. H. Gellman, *J. Am. Chem. Soc.* **2011**, *133*, 7336–7339; c) J. A. Kritzer, O. M. Stephens, D. A. Guarracino, S. K. Reznik, A. Schepartz, *Bioorg. Med. Chem.* **2005**, *13*, 11–16; d) J. W. Checco, E. F. Lee, M. Evangelista, N. J. Sleebs, K. Rogers, A. Pettikiriarachchi, N. J. Kershaw, G. A. Eddinger, D. G. Belair, J. L. Wilson, C. H. Eller, R. T.

Raines, W. L. Murphy, B. J. Smith, S. H. Gellman, W. D. Fairlie, *J. Am. Chem. Soc.* **2015**, *137*, 11365 – 11375; e) C. M. Grison, J. A. Miles, S. Robin, A. J. Wilson, D. J. Aitken, *Angew. Chem. Int. Ed.* **2016**, *55*, 11096 – 11100; *Angew. Chem.* **2016**, *128*, 11262 – 11266; f) J. Fremaux, C. Venin, L. Mauran, R. H. Zimmer, G. Guichard, S. R. Goudreau, *Nat. Commun.* **2019**, *10*, 924.

[7] a) H. Yin, G. Lee, H. S. Park, G. A. Payne, J. M. Rodriguez, S. M. Sebti, A. D. Hamilton, *Angew. Chem. Int. Ed.* **2005**, *44*, 2704 – 2707; *Angew. Chem.* **2005**, *117*, 2764 – 2767; b) A. Kazi, J. Sun, K. Doi, S.-S. Sung, Y. Takahashi, H. Yin, J. M. Rodriguez, J. Becerril, N. Berndt, A. D. Hamilton, H.-G. Wang, S. M. Sebti, *J. Biol. Chem.* **2011**, *286*, 9382 – 9392.

[8] a) G. M. Burslem, H. F. Kyle, A. L. Breeze, T. A. Edwards, A. Nelson, S. L. Warriner, A. J. Wilson, *ChemBioChem* **2014**, *15*, 1083 – 1087; b) J. P. Plante, T. Burnley, B. Malkova, M. E. Webb, S. L. Warriner, T. A. Edwards, A. J. Wilson, *Chem. Commun.* **2009**, 5091; c) I. Saraogi, J. A. Hebda, J. Becerril, L. A. Estroff, A. D. Miranker, A. D. Hamilton, *Angew. Chem. Int. Ed.* **2010**, *49*, 736 – 739; *Angew. Chem.* **2010**, *122*, 748 – 751; d) S. Kumar, A. D. Hamilton, *J. Am. Chem. Soc.* **2017**, *139*, 5744 – 5755; e) A. Barnard, K. Long, D. J. Yeo, J. A. Miles, V. Azzarito, G. M. Burslem, P. Prabhakaran, T. A. Edwards, A. J. Wilson, *Org. Biomol. Chem.* **2014**, *12*, 6794 – 6799.

[9] B. B. Lao, K. Drew, D. A. Guarracino, T. F. Brewer, D. W. Heindel, R. Bonneau, P. S. Arora, *J. Am. Chem. Soc.* **2014**, *136*, 7877 – 7888.

[10] A. Raghuraman, E. Ko, L. M. Perez, T. R. Ioerger, K. Burgess, *J. Am. Chem. Soc.* **2011**, *133*, 12350 – 12353.

[11] a) M. K. P. Jayatunga, S. Thompson, A. D. Hamilton, *Bioorg. Med. Chem. Lett.* **2014**, *24*, 717 – 724; b) T. Flack, C. Romain, A. J. P. White, P. R. Haycock, A. Barnard, *Org. Lett.* **2019**, *21*, 4433 – 4438.

[12] a) I. Huc, *Eur. J. Org. Chem.* **2004**, 17 – 29; b) D.-W. Zhang, X. Zhao, J.-L. Hou, Z.-T. Li, *Chem. Rev.* **2012**, *112*, 5271 – 5316.

[13] a) P. S. Reddy, B. Langlois d'Estaintot, T. Granier, C. D. Mackereth, L. Fischer, I. Huc, *Chem. Eur. J.* **2019**, *25*, 11042 – 11047; b) S. Kumar, M. Birol, D. E. Schlamadinger, S. P. Wojcik, E. Rhoades, A. D. Miranker, *Nat. Commun.* **2016**, *7*, 11412.

[14] E. R. Gillies, F. Deiss, C. Staedel, J.-M. Schmitter, I. Huc, *Angew. Chem. Int. Ed.* **2007**, *46*, 4081 – 4084; *Angew. Chem.* **2007**, *119*, 4159 – 4162.

[15] a) K. Ziach, C. Chollet, V. Parissi, P. Prabhakaran, M. Marchivie, V. Corvaglia, P. P. Bose, K. Laxmi-Reddy, F. Godde, J.-M. Schmitter, S. Chaignepain, P. Pourquier, I. Huc, *Nat. Chem.* **2018**, *10*, 511 – 518; b) V. Corvaglia, D. Carbajo, P. Prabhakaran, K. Ziach, P. K. Mandal, V. Dos Santos, C. Legeay, R. Vogel, V. Parissi, P. Pourquier, I. Huc, *Nucleic Acids Res.* **2019**, *47*, 5511 – 5521.

[16] H. Jiang, J.-M. Léger, I. Huc, *J. Am. Chem. Soc.* **2003**, *125*, 3448 – 3449.

[17] X. Hu, S. J. Dawson, P. K. Mandal, X. de Hatten, B. Baptiste, I. Huc, *Chem. Sci.* **2017**, *8*, 3741 – 3749.

[18] For an overview of α-helix variability, see: D. J. Kuster, C. Liu, Z. Fang, J. W. Ponder, G. R. Marshall, *PLoS ONE* **2015**, *10*, e0123146.

[19] J. Iriondo-Alberdi, K. Laxmi-Reddy, B. Bouguerne, C. Staedel, I. Huc, *ChemBioChem* **2010**, *11*, 1679 – 1685.

[20] B. Baptiste, C. Douat-Casassus, K. Laxmi-Reddy, F. Godde, I. Huc, *J. Org. Chem.* **2010**, *75*, 7175 – 7185.

[21] J. L. Beesley, D. N. Woolfson, *Curr. Opin. Biotechnol.* **2019**, *58*, 175 – 182.

[22] a) D. F. Kreitler, Z. Yao, J. D. Steinkruger, D. E. Mortenson, L. Huang, R. Mittal, B. R. Travis, K. T. Forest, S. H. Gellman, *J. Am. Chem. Soc.* **2019**, *141*, 1583 – 1592; b) D. Mazzier, S. De, B. Wicher, V. Maurizot, I. Huc, *Angew. Chem. Int. Ed.* **2020**, *59*, 1606 – 1610; *Angew. Chem.* **2020**, *132*, 1623 – 1627.

[23] a) C. D. Andrew, S. Bhattacharjee, N. Kokkoni, J. D. Hirst, G. R. Jones, A. J. Doig, *J. Am. Chem. Soc.* **2002**, *124*, 12706 – 12714; b) R. P. Cheng, P. Girinath, R. Ahmad, *Biochemistry* **2007**, *46*, 10528 – 10537.

[24] M. Vallade, P. Sai Reddy, L. Fischer, I. Huc, *Eur. J. Org. Chem.* **2018**, 5489 – 5498.

[25] M. Kudo, V. Maurizot, B. Kauffmann, A. Tanatani, I. Huc, *J. Am. Chem. Soc.* **2013**, *135*, 9628 – 9631.

Manuscript received: September 7, 2020
Accepted manuscript online: September 10, 2020
Version of record online: November 30, 2020